

# Overview of quasi-single helicity experiments in reversed field pinches

P. Martin<sup>1</sup>, L. Marrelli<sup>1</sup>, G. Spizzo<sup>1</sup>, P. Franz<sup>1</sup>, P. Piovesan<sup>1</sup>, I. Predebon<sup>1</sup>, T. Bolzonella<sup>1</sup>, S. Cappello<sup>1</sup>, A. Cravotta<sup>1</sup>, D.F. Escande<sup>1</sup>, L. Frassinetti<sup>1</sup>, S. Ortolani<sup>1</sup>, R. Paccagnella<sup>1</sup>, D. Terranova<sup>1</sup>, the RFX team<sup>1</sup>, B.E. Chapman<sup>2</sup>, D. Craig<sup>2</sup>, S.C. Prager<sup>2</sup>, J.S. Sarff<sup>2</sup>, the MST team<sup>2</sup>, P. Brunzell<sup>3</sup>, J.-A. Malmberg<sup>3</sup>, J. Drake<sup>3</sup>, the EXTRAP T2R team<sup>3</sup>, Y. Yagi<sup>4</sup>, H. Koguchi<sup>4</sup>, Y. Hirano<sup>4</sup>, the TPE-RX team<sup>4</sup>, R.B. White<sup>5</sup>, C. Sovinec<sup>6</sup>, C. Xiao<sup>7</sup>, R.A. Nebel<sup>8</sup> and D.D. Schnack<sup>9</sup>

<sup>1</sup>Consorzio RFX, Associazione Euratom-Enea sulla fusione, Padova, Italy

<sup>2</sup>Department of Physics, University of Wisconsin-Madison, Madison, WI, USA

<sup>3</sup>Division of Fusion Plasma Physics, Royal Institute of Technology, Association Euratom-VR, Stockholm, Sweden

<sup>4</sup>National Institute of Advanced Industrial Science and Technology (AIST), Tsukuba, Japan

<sup>5</sup>Princeton Plasma Physics Laboratory, Princeton, NJ, USA

<sup>6</sup>Center for Plasma Theory and Computation, University of Wisconsin-Madison, Madison, WI, USA

<sup>7</sup>University of Saskatchewan, Canada

<sup>8</sup>Los Alamos National Laboratory, Los Alamos, NM, USA

<sup>9</sup>Science Applications International Corporation, San Diego, CA, USA

E-mail: piero.martin@igi.cnr.it

Received 8 November 2002, accepted for publication 10 September 2003

Published 1 December 2003

Online at [stacks.iop.org/NF/43/1855](http://stacks.iop.org/NF/43/1855)

## Abstract

We report the results of an experimental and theoretical international project dedicated to the study of quasi-single helicity (QSH) reversed field pinch (RFP) plasmas. The project has involved several RFP devices and numerical codes. It appears that QSH spectra are a robust feature common to all the experiments. Our results expand and reinforce the evidence that the formation of self-organized states with one dominant helical mode (Ohmic SH state) is an approach complementary to that of active control of magnetic turbulence to improve confinement in a steady state RFP.

**PACS numbers:** 52.55.Hc, 52.55.Tn, 52.35.Ra, 52.65.Cc, 52.35.Mw

## 1. Introduction

The reversed field pinch (RFP) [1] belongs to the class of toroidal pinch configurations. Like the tokamak, the confining magnetic field has toroidal and poloidal components,  $B_\phi$  and  $B_\theta$ , respectively. Unlike the tokamak, the two components are of the same order of magnitude. This means that, for a given plasma current, the edge magnetic field is an order of magnitude lower than that in the tokamak. In addition, the toroidal field at the edge is in a direction opposite to that in the core. The magnetic field components are both generated mainly by electric currents flowing into the plasma, through a magnetic self-organization process. Part of the electric field to drive these currents is self-generated by the plasma in the so-called ‘dynamo’ process [1].

In the last few years a significant effort of the RFP community has been dedicated to the study of helical RFP states. This is based on the theoretical prediction that the RFP plasma can spontaneously access, through a self-organization process, the single helicity (SH) regime [2]. In this condition the dynamo needed to sustain the RFP configuration is driven by an individual  $m = 1$  saturated resistive kink and has a laminar character. Closed magnetic flux surfaces are preserved in the SH regime. Given the RFP safety factor profile,  $m = 1$  and 0 modes are the most important for the configuration. The SH state is naturally resilient to magnetic chaos and this is beneficial for plasma confinement. Moreover, since SH is the result of a spontaneous chaos–order transition in a complex system, it shares a lot of physics with other natural systems.

The proposition that a RFP plasma could exist in a pure SH state was put forward in 1983, based on two-dimensional numerical simulations (see [3, 2] for a collection of references), where a stationary RFP state was found by forcing SH. Later, the existence of a bifurcation from the standard multi-mode (multiple helicity (MH)) to SH was proved in fully three-dimensional simulations [4–6]. It has been hypothesized recently that this bifurcation is controlled by the Hartmann number  $H \propto (\nu\eta)^{-1}$ , where  $\eta$  and  $\nu$  are the plasma resistivity and viscosity, respectively [3]. The SH states are not the helical Taylor states [2], since the sign of their helical pitch is opposite to that found in Taylor’s theory for  $\Theta > 1.56$  [7].

On the experimental side, since 1994, results have been reported in several machines where the plasma was transiently in a quasi-SH (QSH) state [8–11]. Stationary QSH spectra have been discovered in RFX [12] where, in this regime, a coherent helical structure in the plasma core with closed magnetic flux surfaces has been detected. QSH states are the closest experimental approximation of the theoretical SH states: QSH differs from SH mainly because of the characteristics of the magnetic spectra of  $m = 1$  modes. While one  $m = 1$  mode dominates the QSH spectra, the other modes (the so-called ‘secondary’ modes) still have non-zero amplitude and therefore contribute to the production of residual magnetic chaos outside the coherent helical flux surface structure.

Given the potential benefit of a self-organized, non-chaotic RFP configuration, we have started an experimental and theoretical project, which involves several RFP devices and numerical codes. This initiative is devoted to collect and organize all the QSH evidence in a unique database to study QSH in a variety of different conditions and to control and optimize this helical regime. In this paper, we report the results of this effort.

Experiments have been conducted in four different RFP devices: EXTRAP T2R at the Royal Institute of Technology in Stockholm [13], TPE-RX at AIST in Tsukuba [14], MST at the University of Wisconsin-Madison [15] and RFX at Consorzio RFX in Padova [16]. Their main characteristics are summarized in table 1. Though small, the RFP community can count on experimental devices that are suited to different conditions and cover, therefore, a wide range of operating regimes and boundary conditions. Conditions which might control MHD mode dynamics, such as the aspect ratio, size, current density, plasma density and magnetic boundary, vary significantly in the different devices.

The codes that have been used for this study are ORBIT [17], NIMROD [18], SPECYL [19] and DEBS [20]. ORBIT is a Hamiltonian guiding-centre Monte Carlo code with numerical or analytical equilibria. NIMROD is a three-dimensional MHD code capable of working with generic

geometry, while SPECYL and DEBS are three-dimensional cylindrical MHD codes.

This paper is organized as follows. In section 2 we present an overview of the main experimental results, which describe the QSH regime. Section 3 is dedicated to the measurements of plasma flow velocity fluctuations in QSH conditions. The plasma flow velocity fluctuation  $\tilde{v}$  is an important ingredient for the self-generated dynamo electric field, which is, in general, proportional to  $\tilde{v}$  and to the magnetic field fluctuation  $\tilde{b}$  ( $E_d \propto \langle \tilde{v} \times \tilde{b} \rangle$ ). In section 4 we discuss the experimental parameters, which control the transition to QSH spectra, while a numerical transport and stability analysis of SH states is discussed in section 5. Conclusions are drawn in section 6.

## 2. The QSH experimental picture

QSH plasmas have been studied with a variety of diagnostics. Standard MH spectra of  $m = 1$  MHD resistive kinks in RFPs, measured by pick-up coils, are composed of many modes with various toroidal mode numbers  $n \geq 2(R/a)$ , where  $R$  and  $a$  are the major and minor radii, respectively [1]. The spectrum is usually peaked around the values  $n \approx 2(R/a)$ . In MH conditions several modes have comparable amplitudes, though the amplitude of  $m = 1$  modes rapidly decreases for increasing  $n$ . QSH spectra are characterized by the presence of one ( $m = 1, n = n_D$ ) dominant mode. Its amplitude is typically several times larger than those of the secondary modes. The ratio between the dominant and the secondary mode amplitudes varies depending on the device and is also a function of the plasma conditions, but values  $\geq 3$  typically characterize the QSH spectra. It is customary to describe the width of the toroidal spectrum of  $m = 1$  modes by means of the  $N_s$  parameter, defined as  $N_s = [\sum_n (W_n / \sum_{n'} W_{n'})^2]^{-1}$ , where  $W_n$  is the energy of the ( $m = 1, n$ ) mode. A pure SH spectrum corresponds to  $N_s = 1$ .

Reproducible experimental evidence of spontaneous QSH spectra has been observed in three devices, RFX, MST and TPE-RX. QSH has been detected only sporadically in EXTRAP T2R, though we should point out that a wide plasma parameter scan has not been performed yet in this device. For these devices typical time traces of the amplitudes of the ( $m = 1, n$ ) modes normalized to the edge poloidal magnetic field are shown in figure 1 (for RFX and TPE-RX the toroidal component of the magnetic fluctuation is shown and the poloidal one is shown for MST and EXTRAP T2R). This figure shows some important features about the time evolution and the purity of QSH spectra. QSH spectra lasting throughout the discharge are observed in RFX and TPE-RX (figures 1(a) and (b)), while in MST QSH spectra are typically transient, though lasting for a significant fraction of the plasma pulse (figure 1(c)). A discharge with QSH spectrum in EXTRAP T2R is reported in figure 1(d). In all devices, anyway, the duration of QSH conditions is longer than the standard energy confinement time. In MST the purest spontaneous QSH spectra have been recorded (with the ratio between dominant and secondary mode amplitudes  $> 10$ ). MST shows that the onset of QSH corresponds to a selection process among the various modes. A redistribution of the energy between the modes is in fact observed [21]: the increase of the dominant mode amplitude, when a QSH spectrum is established, is

**Table 1.**

Device	$R/a$ (m)	Plasma current achieved/design (kA)	Vertical field penetration time (ms)
EXTRAP T2R	1.24/0.183	100/300	$\approx 6$
TPE-RX	1.72/0.45	500/1000	$\approx 320$
MST	1.5/0.52	500/500	$\approx 500$
RFX	2/0.457	1100/2000	$\approx 400$

accompanied by a decrease in the amplitude of the secondary modes. A consistent result is obtained also in TPE-RX: figure 2 shows the behaviour of the dominant mode (figure 2(a)) and secondary mode (figure 2(b)) amplitudes for TPE-RX as a function of  $N_s$ . Each point corresponds to an average over several reproducible discharges. A wide enough database has not been collected in T2R yet to check whether a similar behaviour is present in this device too.

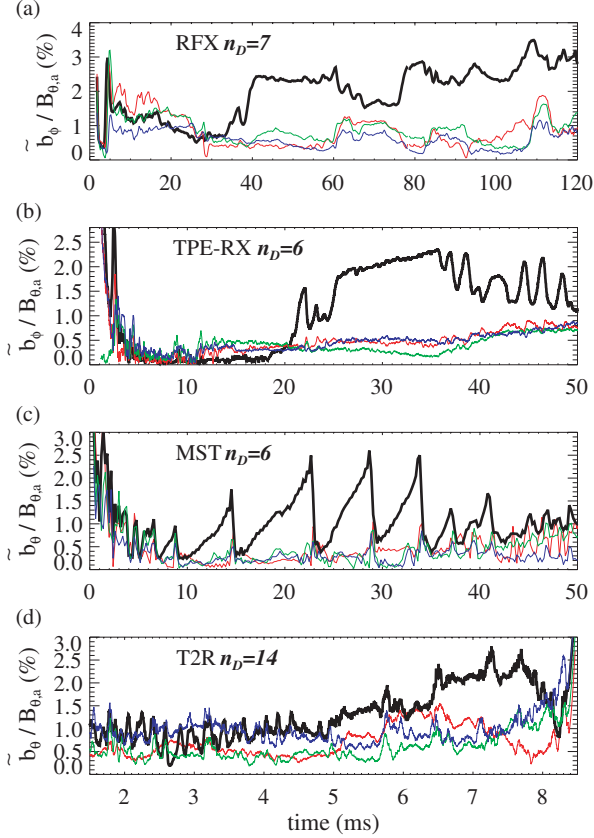


**Figure 1.** Time traces of the  $(m = 1, n)$  mode amplitudes normalized to the edge poloidal magnetic field for the four RFP devices: (a) RFX; (b) TPE-RX; (c) MST; (d) EXTRAP T2R. For RFX and TPE-RX the toroidal component of the magnetic fluctuation is plotted and for MST and EXTRAP T2R the poloidal component is plotted.

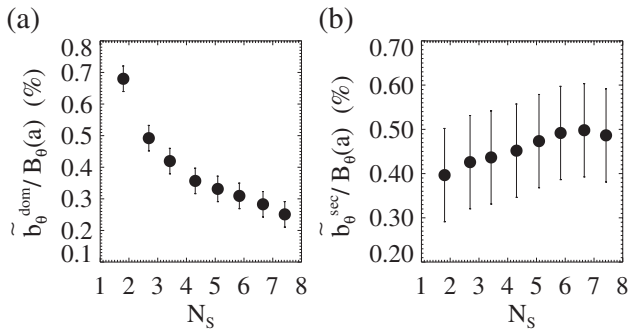


**Figure 2.** (a) Dominant mode amplitude and (b) total amplitude of secondary modes ( $=\sqrt{\sum_{n \neq n_d} b_{\varphi, n}^2}$ ) versus  $N_s$  for TPE-RX. Each point corresponds to an ensemble over several reproducible discharges.

These external magnetic fluctuation measurements are closely correlated with a significant modification of the plasma core. Soft x-ray (SXR) tomographic imaging [12] reveals that the dominant mode produces a helical coherent structure with closed helical flux surfaces and the same pitch as the dominant magnetic mode. For our study, SXR tomography was available in RFX [22] and MST [23]. The maps of SXR emissivity are rather different [22] in QSH plasmas with respect to MH. A poloidally symmetric emissivity is found in the MH state. This is consistent with a region of strong heat transport in the plasma core, as one could expect because of the presence of a stochastic magnetic field [24]. In contrast, a bean-like, hot  $m = 1$  structure is evident in the QSH case. The location of the structure systematically coincides with the resonance radius and poloidal phase angle of the dominant  $m = 1$  mode, which are reconstructed from magnetic measurements [22, 25]. A typical example of coherent structure imaging in MST is shown in figure 3. Imaging has been performed by means of miniaturized SXR cameras recently developed for MST [23]. They allow simultaneous imaging in the poloidal and toroidal directions. This figure shows the island when, due to its rotation, it is located at the low field side (LFS) (figure 3(a)) and at the high FS (HFS) (figure 3(b)) of the torus, respectively. The different sizes of the islands on the LFS and HFS are a result of toroidal effects, which are directly detected in MST with FIR polarimetry [26]. We notice that the structure extends radially for a significant fraction of the minor radius. The global nature of the helical structure is confirmed also by the toroidal SXR camera. The lines of sight of the toroidal array span an angle of  $\approx 30^\circ$  in the toroidal direction. The contour plot in figure 4 shows the time evolution of the SXR brightness profile for the toroidal array. The helical deformation, which rotates at the same velocity of the dominant  $m = 1$  MHD mode, is evident.

These results show that an increased energy stored in magnetic fluctuations does not necessarily mean magnetic stochasticity: the transition from chaos to order is also controlled by the energy distribution among the various modes. This is confirmed by the magnetic flux surface analysis performed with the ORBIT code. The equilibrium magnetic field profiles used in the code are computed from the cylindrical  $\mu$ & $p$  [1] model, and toroidal effects are taken into account by adding a second-order Shafranov shift. The magnetic fluctuation spectrum measured at the plasma edge is used as a boundary condition for the calculation of the radial perturbations  $b_r$ . This is done by solving the Newcomb equation: a regularity condition on the magnetic axis and the

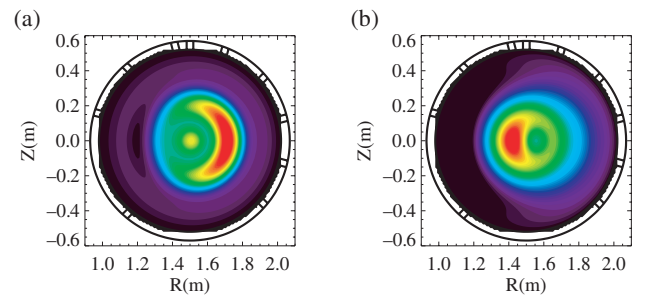


**Figure 3.** A typical example of coherent structure SXR imaging in MST. This figure shows the island when, due to its rotation, it is located at the LFS (a) and at the HFS (b) of the torus, respectively.

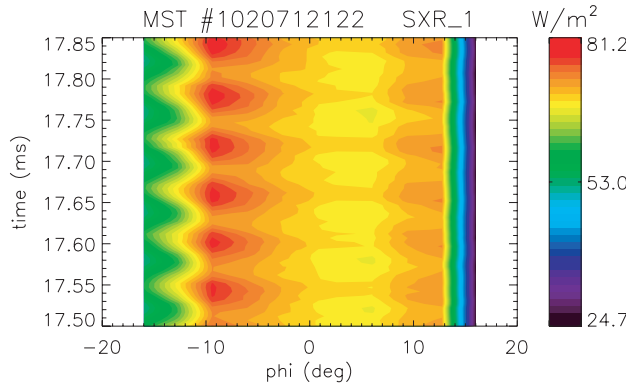


**Figure 4.** Time evolution of the SXR brightness profile for the toroidal SXR array in the MST device. The  $x$ -axis represents the toroidal impact angle of each line of sight. Brightness is measured in  $\text{W m}^{-2}$ .

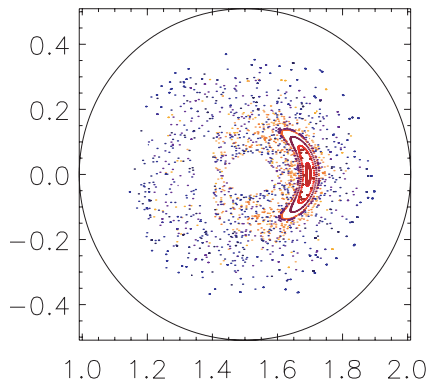


**Figure 5.** Poincaré plot in the poloidal cross section calculated with the ORBIT code for a MST QSH spectrum with  $n_D = 6$ , corresponding to the same 400 kA shot as in figure 3. The radial coordinate  $R$  (in m) is on the  $x$ -axis and the vertical spatial coordinate is on the  $y$ -axis.

continuity of the solutions, with the exception of the first derivative, are imposed at the rational surface. In the RFX case the vacuum region between the vacuum container and the conductive shell is also taken into account (the shell is located at  $r \approx 1.17 \times r_{\text{wall}}$ ). Figure 5 shows a Poincaré plot in the poloidal cross section calculated from realistic magnetic equilibrium and mode radial eigenfunctions for the same MST 400 kA shot of figure 3, corresponding to a spontaneous QSH spectrum with  $n_D = 6$ . We note in figure 5 that a coherent structure emerges from magnetic chaos. For the case shown in the figure this leads to a peak amplitude of the radial magnetic field fluctuation associated to the dominant mode of  $\approx 0.01 B(0)$  (where  $B(0)$  is the on-axis magnetic field), i.e.  $\approx 6$  mT.

As a final point, it is worth noting the beneficial effects of QSH spectra on the mode wall-locking problem, which affects in particular RFX and TPE-RX. In RFX, wherein MH conditions modes are always strongly locked among themselves and to the wall, the strength of the phase correlation between  $m = 1$  modes is reduced in QSH conditions, as shown in figure 6. Here, the distribution of locking strength values  $L_S$  is reported for MH and QSH plasmas [27].  $L_S$  is defined as the normalized sum over the main interacting modes of the cosine of their phase difference  $L_S \propto \sum_{n_1, n_2} \cos(\varphi_{n_1} - \varphi_{n_2})$ . A perfect phase locking gives a value of  $L_S = 1$ , while a

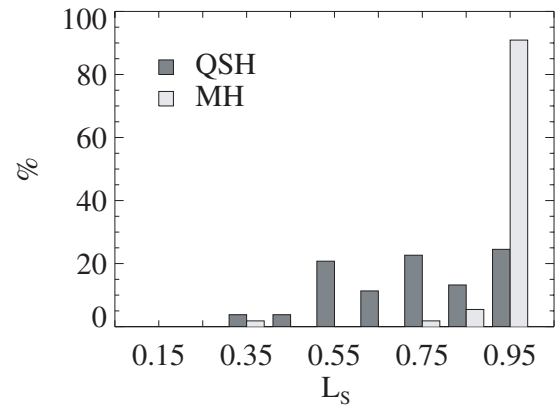


**Figure 6.** Distribution of locking strength values  $L_S$  for MH and QSH plasmas in RFX.

complete decorrelation gives a value equal to 0. We observe that in MH conditions practically all the plasmas have almost complete phase locking ( $L_S \approx 1$ ). In QSH conditions the distribution is wider, and lower values of  $L_S$  are found with significant probability. The reduction of phase locking is often associated to the onset of a spontaneous rotation of one or two  $m = 1$  modes, typically with  $n$  numbers close to that of the dominant one. This is due to a redistribution of the magnetic energy between the various normal modes as a result of the MH to QSH transition and to a modified non-linear interaction between modes [27]. RFX results also show that wall-locking of the dominant mode in QSH conditions has milder effects on the plasma-wall interaction in comparison with what happens in MH [12].

### 3. Velocity and magnetic fluctuations during QSH

Numerical simulations indicate that a RFP configuration can be sustained with a single  $m = 1$  mode in a pure SH state. Although this condition has not been achieved experimentally, it is important to determine whether the dominant mode in QSH plasmas produces significant dynamo fields of the form  $\vec{E}_d = \langle \vec{v} \times \vec{b} \rangle$ , where  $\langle \dots \rangle$  represents a flux surface average. Previous work in MST reported that in standard MH sawtooth plasmas, the dynamo action was large only during sawtooth crashes, when large amplitude magnetic and velocity fluctuations with a broad spectrum were coherent and in the proper phase to produce a  $(\vec{v} \times \vec{b})$  electric field [28].

For this study, the poloidal component of plasma flow velocity fluctuations  $\vec{v}$  have been measured in MST at 300 kA, far from sawtooth events, with Doppler spectroscopy [29] along five parallel chords in a poloidal cross section and along one toroidal line of sight. From these measurements two ensembles, one with points corresponding to MH plasmas and one with points corresponding to QSH plasmas, have been assembled. Each point in the ensemble corresponds to an average over 0.5 ms. By correlating  $\vec{v}$  measurements with mode resolved edge magnetic field fluctuations, the coherent part of the velocity fluctuations associated with individual ( $m = 1, n$ ) modes have been isolated for each line of sight. In figure 7, the radial profile of contribution to the velocity fluctuation from the  $n = 6$  mode (triangles) during QSH (figure 7(a)) and MH (figure 7(b)) is compared to the average

contribution from all of the secondary modes (squares). Each point in the profiles corresponds to a different line of sight (identified by its impact parameter). We observe that the velocity fluctuation for the dominant  $n = 6$  mode increases during QSH, together with the increase in magnetic fluctuation amplitude for the same mode. Also, the velocity fluctuation for other modes stays the same or decreases in QSH. This implies that the velocity fluctuations have achieved a narrower spectrum in a similar way to the magnetic fluctuations. This is confirmed in figure 8: in (a) and (b) the ensemble average spectra of  $m = 1$  magnetic fluctuations for MH and QSH conditions are shown. In figures 8(c) and (d) we show the

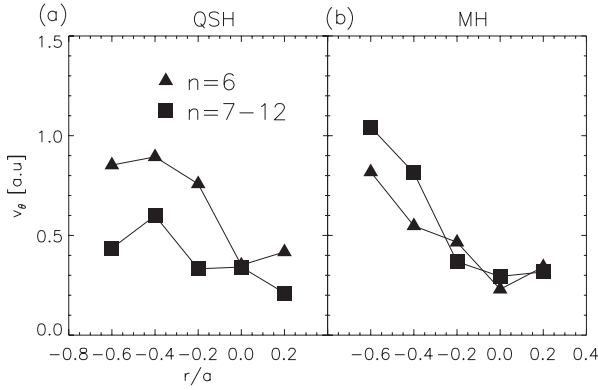


**Figure 7.** The contribution to plasma flow velocity fluctuations from the  $n = 6$  mode ( $\blacktriangle$ ) in several radial positions (corresponding to the available lines of sight of the spectrometer) is compared to the average from all the secondary modes with  $n = 7-12$  ( $\blacksquare$ ) during QSH (a) and MH (b).

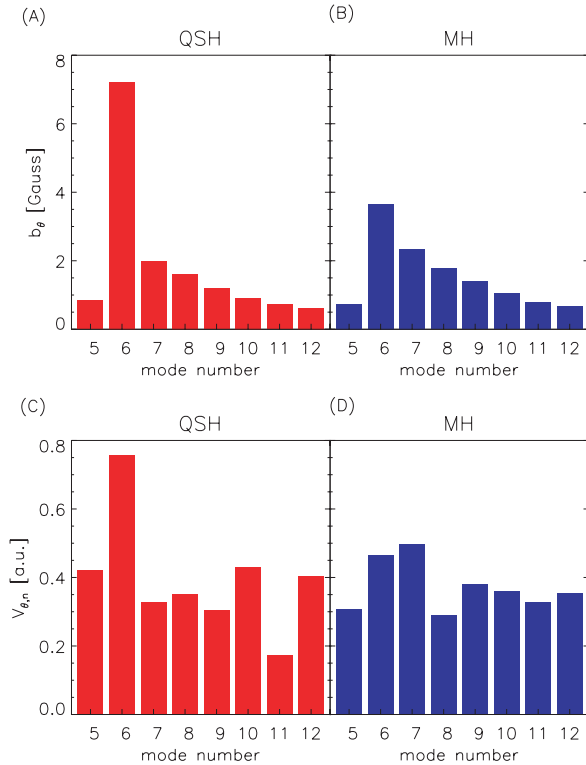


**Figure 8.** Toroidal mode number,  $n$ , spectrum of magnetic fluctuations: (a) for QSH and (b) for MH; plasma flow velocity fluctuations: (c) for QSH and (d) for MH.

ensemble averaged spectra of the coherent part of the velocity fluctuations associated with individual  $(1, n)$  modes, measured at  $r = -0.2a$  in QSH and MH conditions (minus sign means that the line of sight is on the inboard side of the poloidal cross section of the torus). Work is continuing on extracting the dynamo product  $\langle \tilde{v} \times \tilde{b} \rangle$  from these data. However, it seems likely (and supported by preliminary analysis) that the dynamo produced by the dominant  $n = 6$  mode will be significantly larger during QSH than what is observed away from sawteeth in MH.

#### 4. QSH experimental control parameters

The large data sets of reproducible discharges obtained in the four devices has enabled a statistical analysis of QSH spectra, and the search for their experimental control parameter. Numerical studies show that the MH–SH transition is ruled by the Hartmann number  $H$ . Given the difficulty of an accurate measurement of plasma viscosity, a direct comparison with the theory is very difficult. Therefore, we concentrated on experimental global plasma control parameters. Analyses performed in MST [21], RFX [27] and TPE-RX shows some common trends. In all three devices we observe a trend for an increased probability of obtaining QSH spectra when the current is raised. Figure 9(a) shows the probability density function  $p(N_s)$  of  $N_s$  values for different values of plasma current in TPE-RX.  $p(N_s)$  is normalized such that  $\int p(N_s) dN_s = 1$ . Low values of  $N_s$  are more likely at the higher current levels. It is worth noting that this experimental trend for the probability of QSH to increase with plasma current is difficult to reconcile with the theoretical Hartmann scaling [3], given the present knowledge. In fact, the latter predicts that SH is achieved when dissipation in plasma is increased, a condition that is hardly achieved in higher plasma current, higher temperature regimes.

Not only the absolute value of the plasma current, but also its time evolution might influence the spectral shape. We know in fact that a QSH spectrum is achieved in numerical simulations during current ramp-down experiments [30].

The shape of the magnetic equilibrium and in particular the amount of edge magnetic toroidal field reversal also influences the probability of obtaining QSH spectra: QSH spectra are more frequently observed in discharges with shallow reversal, as indicated in figure 9(b), where the  $p(N_s)$  function is shown for two different values of  $F = B_\psi(a)/\langle B_\psi \rangle$ .

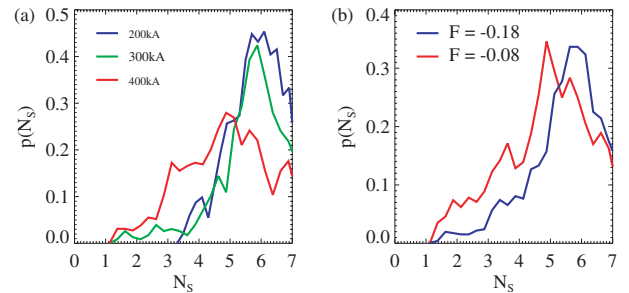


**Figure 9.** Probability density function  $p(N_s)$  of  $N_s$  values in TPE-RX (a) for different values of the plasma current ( $I_p = 200, 300, 400$  kA) at fixed reversal parameter  $F$  and (b) for different values of  $F$  ( $F = -0.18, -0.08$ ) at fixed plasma current.

A similar result is found in RFX [27]. This is consistent with numerical results from the SPECYL code applied to RFX geometry: they indicate that at shallow reversal the MH–SH transition threshold (as a function of  $H$ ) is smoother [31]. This corresponds to a wider QSH transition range with less negative  $F$ , which means that corresponding to the case of  $H$  values where at deep  $F$  a MH spectrum is still found, QSH spectra are observed at shallower  $F$ .

The aspect ratio is also a parameter that influences the shape of the MHD mode spectrum. It is known [32] that the average number of  $m = 1$  modes in the spectrum depends on the aspect ratio. This might explain the less frequent QSH spectra in EXTRAP T2R, which is the device with the larger aspect ratio (table 1): here, the background standard  $m = 1$  spectrum is broad, and the plasma must strongly depart from the standard spectrum in order to get QSH conditions. For the lower aspect ratio MST device, standard spectra are on the average rather narrow.

The SH could be obtained by a direct control of the MHD spectrum through properly powered active coils. The results of numerical simulations [33], which show that active feedback control of internal modes in the RFP is possible, are very encouraging. The dominant, near-axis resonant,  $m = 1$  mode has been driven and controlled in the simulation [33] both for plasma parameters corresponding to relatively high and low viscous dissipation, i.e. for plasmas that are naturally evolving towards SH or MH states, respectively. This opens a path for actively driving SH starting from a standard MH target plasma. Significant experiments on this and related topics will be performed in the renewed RFX device, which will be

equipped with 48 (toroidal)  $\times$  4 (poloidal) active coils, each individually driven. This system, together with improved diagnostic capabilities, will allow important experiments on active control of MHD modes.

## 5. Confinement and stability in finite- $\beta$ helical states

Experimental measurements [12, 34] show that the helical coherent structure is a region of reduced transport. SXR emissivity is stronger and direct measurements show that the electron temperature in the island is indeed larger there than in the surrounding plasma [34]. Given the limited volume of the helical structure (e.g. in RFX up to 10% of the total plasma volume), the global confinement is not strongly affected. It is worth noting that in MST, where the purest QSH spectra are obtained and the more marked reduction of secondary modes is recorded, we observe an increase of SXR emission from the plasma core when a QSH mode spectrum is present [21].

In order to model the observed confinement changes in QSH spectra and to predict what would happen if a pure SH could be reached, we have performed a study of particle transport with the ORBIT code. This has been done by analysing the diffusion of an ensemble of monoenergetic test particles (ions), which have been deposited in the plasma core in three different magnetic configurations: MH, QSH and SH. All these configurations have the same total magnetic energy stored in  $m = 1$  modes, but distributed in different ways among the various helicities. The resulting toroidal Poincaré plots for the three configurations are shown in figure 10. We clearly note the good flux surfaces all across the plasma in

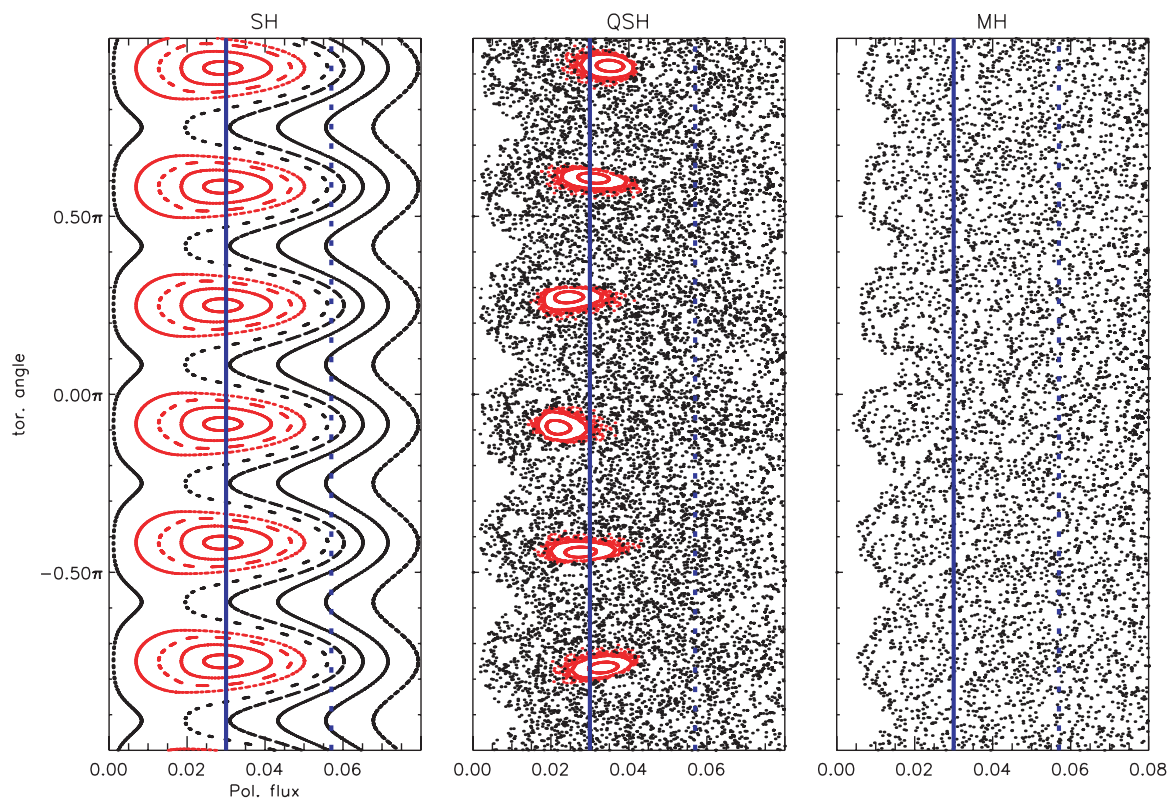


**Figure 10.** The toroidal Poincaré plots for the three configurations (MH, QSH and SH) used for particle loss time studies. The solid line represents the deposition line and the dashed line the border, which the particles have to cross.

the SH conditions. Particle transport properties have been investigated by means of Monte Carlo methods. As a first approximation, for the treatment of monoenergetic particle distributions, collisions have been taken to be elastic (energy conserving). The Lorentz collision operator for pitch angle scattering has been modelled as in Boozer and Petravac [35]. As neoclassical transport in the RFP gives only a negligible enhancement over the classical value (banana widths in RFP geometry may be comparable or smaller than the gyroradius and even vanish at the reversal surface), we have added to the simulation a collision operator that includes a random displacement of a particle by a gyroradius in one collision time. In those parts of the discharge where radial drifts are important the neoclassical transport dominates and this classical diffusion is negligible.

To quantify the transport, we have computed the time needed to lose 50% of the particles deposited in the plasma core (at a radial location, which in SH corresponds to that of the helical structure) out from a preset border located at an outer radius. The computation has been repeated several times, depositing each time the test particles in a different toroidal position along the deposition line. In figure 10 the deposition line and the border are shown. We find that particles deposited inside the helical structure in the QSH case are lost more slowly than those deposited outside it or in a MH plasma. The loss time in the former case is about one order of magnitude longer. A further one order of magnitude improvement with respect to QSH is found with a pure SH spectrum, when particles are deposited inside the helical structure. In this case no magnetic chaos is present outside the helical domain. These results are summarized in figure 11, where the loss times for MH, QSH and SH configurations are shown as a function of the toroidal location where the particles are deposited.

The investigation of some stability properties of finite- $\beta$  SH states has been performed by means of the NIMROD code. The pressure gradient maintained in the helical region represents in fact a source of free energy for MHD modes, but the longevity of the temperature distortions suggests that pressure-driven modes may be stable. Although axisymmetric RFP equilibria have bad magnetic curvature everywhere and

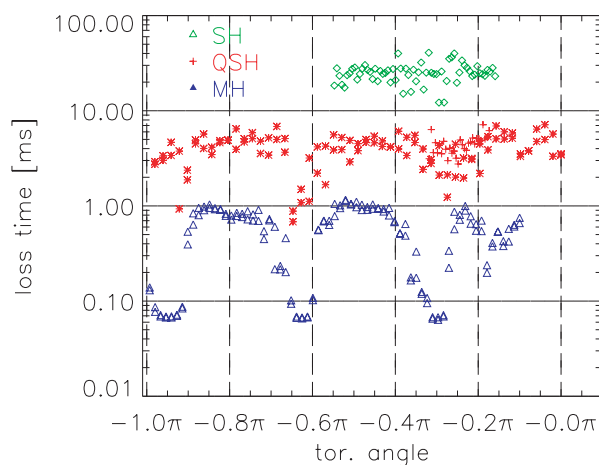


**Figure 11.** Particles loss time versus the toroidal position where the test particles start, for the MH, QSH and SH configurations of figure 10.

are, therefore, susceptible to resistive pressure-driven modes, the helical flux surfaces in SH and QSH states have distinct topologies that resemble stellarator-like configurations.

The finite- $\beta$  properties of SH and QSH states are being investigated numerically with the NIMROD code [18]. The geometry for the computations is a periodic cylinder, which allows the formation of pure SH states, and the parameters  $S = 2000$  and  $Pm = 100$  are chosen to produce SH, as expected from a study at  $\beta = 0$  [3].  $S$  and  $Pm$  are the Lundquist and Prandtl numbers, respectively. With Ohmic heating and anisotropic thermal conduction (leading to internal energy  $\approx 15\%$  of the stored energy), the resulting pressure distribution is peaked at the magnetic axis of the helical flux surfaces, which remain intact. The computed temperature distribution (figure 12(a)) has features that resemble the experimental SXR measurements displayed in figure 3. The flux-surface-averaged magnetic pressure from the simulation (figure 12(b)) shows the existence of a magnetic well [36] from the helical magnetic axis ( $r_0 = 0.45$ ) to the separatrix ( $r_0 = 0.68$ ), where  $r_0$  is a Lagrangian coordinate. Although the well is suggestive of good average curvature, it does not prove MHD stability. The large viscosity needed for

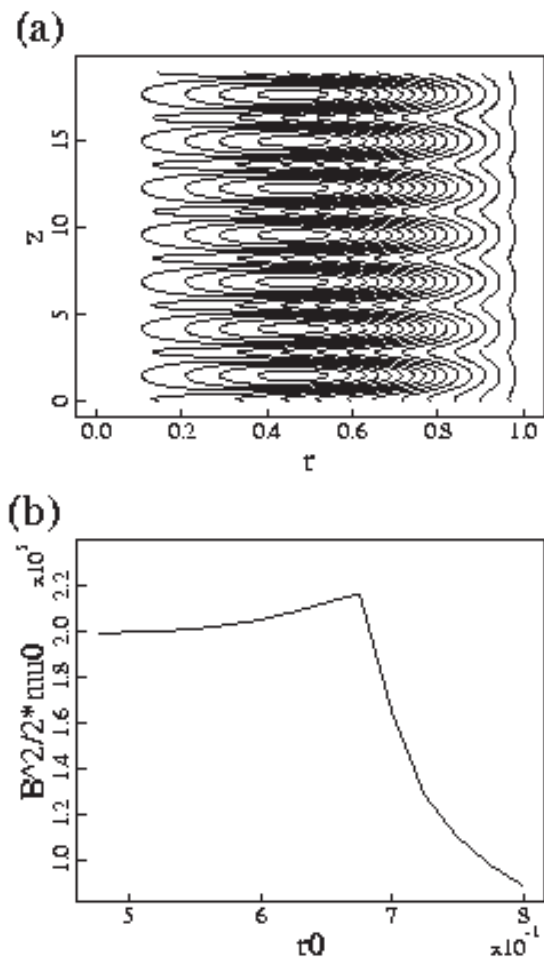


**Figure 12.** Results of a NIMROD simulation for a finite- $\beta$  SH case: (a) the computed two-dimensional temperature distribution plotted as a function of the radial coordinate  $r$  and of the toroidal coordinate  $Z$  and (b) the flux-surface-averaged magnetic pressure  $B^2/2\mu_0$  versus the radial coordinate.

SH also affects interchange modes and may be the dominant stabilizing effect in the simulation. Nonetheless, the existence of a well is a favourable topological feature of the helical state that is precluded in axisymmetric RFPs.

## 6. Conclusions

This joint international research programme on self-organized helical RFP states has combined the effort of many experimental and theoretical groups. Self-organized QSH spectra are found in all the existing RFP devices: QSH appears, therefore, to be robust and not dependent on very peculiar boundary conditions or magnetic front-end. Most of the experimental QSH features are general and device-independent. The helical coherent structure observed in QSH conditions is numerically reconstructed from realistic magnetic equilibrium and magnetic mode eigenfunctions. When the magnetic modes attain a QSH spectrum, the plasma flow velocity fluctuations also achieve a narrower spectrum. This suggests that the dynamo produced by the dominant mode is significantly larger during QSH than what is observed away from sawteeth in MH. Global plasma parameters, which favour the transition towards QSH spectra, have been identified. In particular, it is encouraging to note that QSH states are experimentally more easily accessible at high plasma current.

Long lasting QSH states have been found in several experiments. This, along with the experimental hints of a more steady dynamo action provided by the dominant mode as compared to the intermittent nature typical of the MH dynamo, are suggestive signatures of a path towards a laminar dynamo field as predicted by pure SH numerical states. The reduced plasma-wall interaction, and the observed heating of the helical structure, are also promising features for the future optimization and full exploitation of helical states in RFPs. Numerical simulations show that the good particle confinement properties and the existence of a magnetic well are distinctive features of helical RFPs, when compared to the standard axisymmetric mean field profiles with a MH magnetic turbulence.

The results of numerical simulations, which show that active feedback control of internal modes in the RFP is possible, indicate a path for active induction of SH states even starting from a standard MH target plasma. The renewed RFX device will be a very useful tool for this study.

Although much remains to be done, our results expand and reinforce the evidence that the formation of self-organized states with one dominant helical mode (Ohmic SH state) is an approach complementary to that of active control of magnetic turbulence to improve confinement in a steady state RFP.

## Acknowledgment

This work is being carried out in the framework of the IEA Implementing Agreement on Reversed Field Pinches.

## References

- [1] Ortolani S. and Schnack D.D. 1993 *Magnetohydrodynamics of Plasma Relaxation* (Singapore: World Scientific)
- [2] Escande D.F. *et al* 2000 *Plasma Phys. Control. Fusion* **42** B243–53
- [3] Cappello S. and Escande D.F. 2000 *Phys. Rev. Lett.* **85** 3838
- [4] Cappello S. and Paccagnella R. 1990 *Proc. Workshop on Theory of Fusion Plasmas* ed E. Sindoni (Bologna: Compositori) p 595
- [5] Cappello S. and Paccagnella R. 1992 *Phys. Fluids B* **4** 611
- [6] Finn J.M., Nebel R.A. and Bathke C.C. 1992 *Phys. Fluids B* **4** 1262
- [7] Taylor J.B. 1974 *Phys. Rev. Lett.* **33** 1139
- [8] Nordlund P. and Mazur S. 1994 *Phys. Plasmas* **1** 4032
- [9] Brunzell P. *et al* 1993 *Phys. Fluids* **5** 885
- [10] Sarff J.S. *et al* 1997 *Phys. Rev. Lett.* **78** 62
- [11] Martin P. 1999 *Plasma Phys. Control. Fusion* **41** A247
- [12] Escande D.F. *et al* 2000 *Phys. Rev. Lett.* **85** 1662
- [13] Brunzell P.R. *et al* 2001 *Plasma Phys. Control. Fusion* **43** 1457–70
- [14] Yagi Y. *et al* 1999 *Fusion Eng. Des.* **45** 409
- [15] Dexter R.N. *et al* 1991 *Fusion Technol.* **19** 131
- [16] Rostagni G. 1995 *Fusion Eng. Des.* **25** 301
- [17] White R.B. 1990 *Phys. Fluids* **2** 845
- [18] Glasser A.H. *et al* 1999 *Plasma Phys. Control. Fusion* **41** A747
- [19] Cappello S. and Biskamp D. 1996 *Nucl. Fusion* **36** 571
- [20] Schnack D.D. *et al* 1986 *Comput. Phys. Commun.* **43** 17
- [21] Marrelli L. *et al* 2002 *Phys. Plasmas* **9** 2868
- [22] Franz P. *et al* 2001 *Nucl. Fusion* **41** 695–709
- [23] Franz P. *et al* 2003 *Rev. Sci. Instrum.* **74** 2152
- [24] Intravaia A. *et al* 1999 *Phys. Rev. Lett.* **83** 5499–502
- [25] Spizzo G. *et al* 2001 *Plasma Phys. Control. Fusion* **43** L17–22
- [26] Brower D. *et al* 2002 *Proc. 19th Int. Conf. on Fusion Energy 2002 (Lyon, 2002)* (Vienna: IAEA) paper EX/C4-6, CD-ROM file, and <http://www.iaea.org/programmes/rip/physics/fec2002/html/node102.htm#25374>
- [27] Bolzonella T. and Terranova D. 2002 *Plasma Phys. Control. Fusion* **44** 2569–81
- [28] Fontana P.W. *et al* 2000 *Phys. Rev. Lett.* **85** 566
- [29] Den Hartog D.J. *et al* 1999 *Phys. Plasmas* **6** 1813
- [30] Nebel R. *et al* 2002 *Phys. Plasmas* **9** 4968
- [31] Cappello S. *et al* 2001 *28th EPS Conf. on Control. Fusion and Plasma Phys.* vol 25A, pp 1553–6
- [32] Ho W. *et al* 1995 *Phys. Plasmas* **2** 3407
- [33] Paccagnella R. 2003 Nonlinear MHD simulations for the RFP with active feedback *Theory of Fusion Plasmas: Proc. of the joint Varenna–Lausanne International Workshop (Varenna, 2002)* vol ISPP-20 (Bologna, Italy: Societa' Italiana di Fisica) p 73
- [34] Martin P. *et al* 1999 *Phys. Plasmas* **7** 1984–92
- [35] Boozer A. and Kuo-Petraivic G.K. 1981 *Phys. Fluids* **24** 851
- [36] Miller G. 1989 *Phys. Fluids B* **1** 384